Available online at www.sciencedirect.com
ScienceDirect
Comput. Methods Appl. Mech. Engrg. 364 (2020) 112929
Computer methods in applied mechanics and engineering
www.elsevier.com/locate/cma

Efficient multiscale modeling for woven composites based on self-consistent clustering analysis☆

Xinxing Han[a,b,1], Jiaying Gao[a], Mark Fleming[a], Chenghai Xu[b], Weihua Xie[b], Songhe Meng[b], Wing Kam Liu[a,*]

[a] Department of Mechanical Engineering, Northwestern University, Evanston, IL 60208, USA
[b] National key Laboratory of Science and Technology on Advanced Composites in Special Environments, Harbin Institute of Technology, Harbin, 150001, China

Received 17 July 2019; received in revised form 26 November 2019; accepted 12 February 2020
Available online 4 March 2020

Abstract

Multiscale simulation of woven composites structure remains a challenge due to extremely expensive computational cost for solving the nonlinear woven Representative Volume Element (RVE). Recently, an effective and efficient Reduced Order modeling method, namely Self-consistent Clustering Analysis (SCA), is proposed to solve the RVE problem. In this work, the curse of computational cost in woven RVE problem is countered using the SCA, which maintains a considerable accuracy compared with the standard Finite Element Method (FEM). The Hill anisotropic yield surface is predicted efficiently using the woven SCA, which can accelerate the microstructure optimization and design of woven composites. Moreover, a two-scale FEM×SCA modeling framework is proposed for woven composites structure. Based on this framework, the complex behavior of the composite structures in macroscale can be predicted using microscale properties. Additionally, macroscale and mesoscale physical fields are captured simultaneously, which are hard, if not impossible, to observe using experimental methods. This will expedite the deformation mechanism investigation of composites. A numerical study is carried out for T-shaped hooking structures under cycle loading to illustrate these advantages.

Keywords: Multiscale simulation; Woven composites; Self-consistent clustering analysis; Reduced order model

1. Introduction

Woven composites are widely used in industries such as the aerospace and automotive industries [1,2] because of their robust mechanical performance. However, performing structural analysis of woven composites is challenging due to the mesoscale and microscale heterogeneities (see Fig. 1). Unique features can be observed at these different scales, and simply homogenizing the composite structure and applying a phenomenological constitutive relationship that only characterizes the average behavior of the material does not account for the localized behavior at the finer

☆ All work presented in this paper are performed at Northwestern University.
* Corresponding author.
E-mail address: w-liu@northwestern.edu (W.K. Liu).
1 Visiting Student at Department of Mechanical Engineering, Northwestern University, Evanston, IL 60208, USA

https://doi.org/10.1016/j.cma.2020.112929

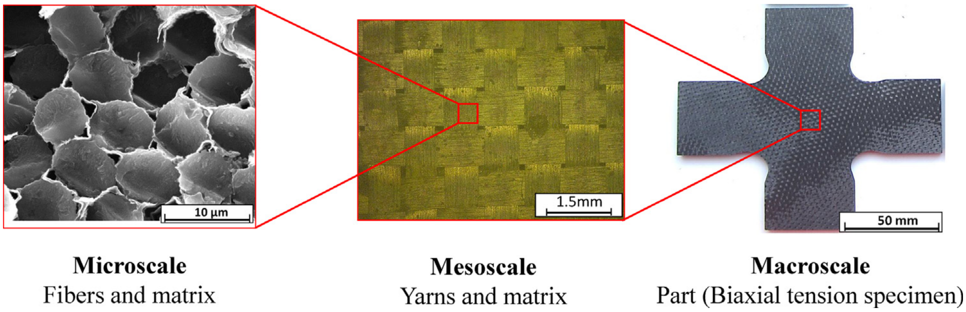

Fig. 1. Multiscale features of woven composites from microscale to macroscale.

scales. As a result, local nonlinear deformation and damage effects are not considered. In addition, the macroscale properties cannot be predicted based on the microstructural constituents, and experiments are required to design new composites, which are costly and time consuming.

Multiscale simulation [3–9] provides a powerful method for analyzing both the material microstructure and macrostructure. Using this method allows the macroscale performance of woven composites to be predicted based on the properties of the constituents. Once the microstructure is characterized, macrostructural experiments are not needed every time the microstructure is changed. This allows the multiscale method to accelerate material design of woven composites, while reducing the cost and improving the analysis accuracy of woven composite structures. Moreover, detailed analysis of the physical fields in different scales is also possible, which is difficult to achieve using experimental methods. Accomplishing effective multiscale simulations for woven composites still involves some challenges, as outlined in the following.

1.1. Challenge 1: efficient woven Representative Volume Element (RVE) solution

Effective macroscale properties are homogenized properties of composites, which are always adopted for the material selection and structural design with woven composites. To predict these effective properties, an RVE [10–14] for the woven composite material must be developed, which will establish the link between the microstructural features and effective macrostructural properties. In the case of a periodic woven architecture, a unit cell is used for the RVE. For the microstructure design, the woven RVE solution can be integrated into an optimization algorithm in which the RVE has to be solved repeatedly to find the optimized solution and satisfy the requirement of effective properties. Therefore, solving the woven RVE problem efficiently can accelerate the whole process of optimization. As a result, it will promote the microstructure design of woven composites.

Currently, several approaches have been proposed for solving the RVE problem. The analytical approaches, such as mixtures rules and theoretical micromechanics methods [15–19], are efficient, but will lose accuracy in the case of complex microstructure and nonlinear, history-dependent material laws. The Direct Numerical Simulation (DNS) method, such as FEM, is extremely time consuming [7]. The Fast Fourier Transform (FFT)-based method [20,21] is more efficient than FEM, but encounters convergence problems for the high phase contrast in nonlinear problems. The Transformation Field Analysis (TFA) [22,23], the Nonuniform Transformation Field Analysis (NTFA) [24–26] and Proper Orthogonal Decomposition (POD) [27–30] are other solution methods, but they require extensive *a priori* simulations to obtain deformation modes, especially for nonlinear phase behavior.

1.2. Challenge 2: concurrent multiscale simulation for woven structures

The behavior of woven composite structures is predicted using the behavior of the RVEs through the concurrent multiscale simulation. Additionally, the physical fields in different involved scales can be captured simultaneously, which will expedite the deformation mechanism investigation of woven composite structures.

Concurrent simulation requires numerous RVE solutions, which is computationally expensive using the FE^2 [7,31] framework, as shown in Fig. 2. In this example, only 5000 elements are used at the macroscale level, 1,843,200 elements are used at the woven RVE mesoscale level. For the concurrent multiscale simulation, every

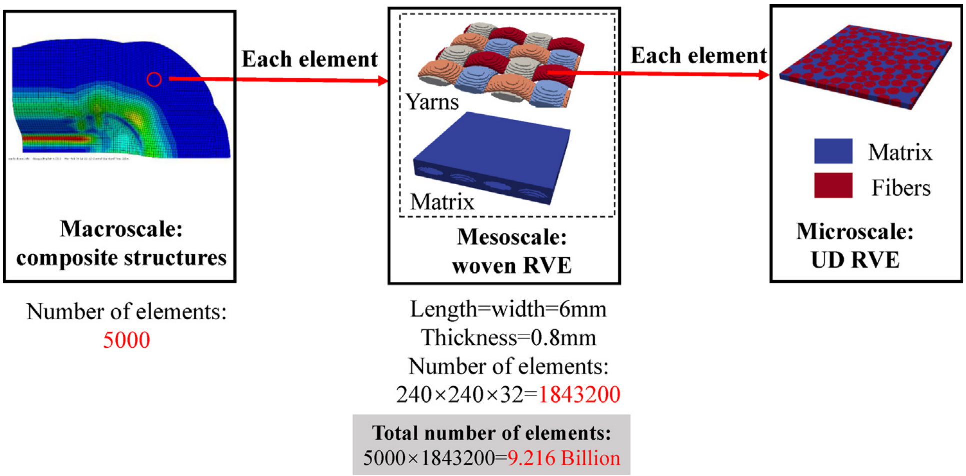

Fig. 2. Multiscale computational challenge of woven composite structures.

up-scale material point will be linked with a down-scale RVE. In this example, assuming a single integration point for each element, 9.216 billion elements are required for the entire multiscale computation. This computation is extremely expensive and would require the use of a High-Performance Computing Cluster (HPCC).

1.3. Solutions for the Challenges 1 and 2

Solving Challenges 1 and 2 requires improving the solution efficiency of the RVE problem. The Self-consistent Clustering Analysis (SCA) proposed by Liu et al. [32] is an effective and efficient method to solve the RVE problem, which can be used for complex woven architecture undergoing irreversible processes, such as inelastic deformation. This makes it particularly attractive for integration into a multiscale simulation. The SCA method involves a two-stage process, an offline stage and an online stage. In the offline stage, a clustering algorithm is used to reduce the overall degrees of freedom (DOF) of the RVE, resulting in a reduced order RVE. In the online stage, the reduced order RVE is utilized for solving the discrete incremental Lippmann–Schwinger integral equation to obtain the stress and strain fields in the reduced order RVE. This efficient method has been used for simulation for 2-dimensional (2D), two-phase composites, and 3-dimensional (3D), hard inclusion material considering nonlinear, elastoplastic damage softening effect [33] and computation for polycrystal material [34]. Additionally, Bessa et al. [35] used this method for data mining and uncertainty analysis. These simulations have demonstrated good efficiency and accuracy.

In this paper, the reduced order modeling process of woven composites by SCA is discussed and the results are compared with FEM. Moreover, the multiscale framework of woven composites is presented for a woven composite. Based on this framework, the part scale mechanical response, whether linear or nonlinear, can be predicted efficiently only using the fiber material and matrix material laws.

This paper is organized as follows: in Section 2, the SCA scheme for woven composites is developed and the concurrent multiscale framework is presented for woven composite structures. In Section 3, the plain weave composites are presented as an example to construct the woven RVE architecture. The nonlinear plasticity model is implemented for an epoxy matrix material. Verification of reduced woven RVE is performed by comparing simulation results obtained from SCA and FEM. In Section 4, the Hill effective anisotropic yield surface is efficiently predicted based on the properties of the constituents, and T-shaped hooking structure made of woven composites is analyzed using proposed FEM×SCA multiscale simulation framework numerically. Additionally, the capacity and advantages of the FEM×SCA multiscale simulation framework are demonstrated in this section. Concluding remarks are provided in Section 5.

1. Mesh the macroscale woven composites part using FEM
2. Begin solution increments
3. Compute integration point field variable from nodal values
4. **for $i = 1$, N_IP** (Loop over integration points)

   a. The macroscale strain increment $\Delta \mathbf{E}$ is passed to user-defined subroutine as input data
   b. Run online part of SCA to solve woven RVE subjected to $\Delta \mathbf{E}$ using offline woven database
   c. Compute the mesoscale strain increment $\Delta \mathbf{e}$ in every cluster in woven RVE domain
   for $j = 1$, N_CLU (Loop over all clusters in this corresponding woven RVE)
   Compute mesoscale stress increment $\Delta \boldsymbol{\sigma}$ using corresponding material model.
   end for (Obtain the response at all clusters)
   d. Check convergence of the reduced-order discrete incremental Lippmann–Schwinger integral equation, if not, update $\Delta \mathbf{e}$ using Newton–Raphson method and go to c, if yes, go to e.
   e. Compute macroscale stress increment $\Delta \boldsymbol{\Sigma}$ by averaging $\Delta \boldsymbol{\sigma}$ in woven RVE domain and pass the macroscale stress back to the FEM solver.

5. **end for** (Obtain the response at all integration points)
6. Check convergence of the FEM part, if not, update nodal values and go to 3

Box I. Flowchart for the concurrent multiscale simulation of woven composite structures.

2. Methodology and framework

2.1. SCA method for a woven RVE at the mesoscale level

A woven composite material is constructed by interweaving yarns in two directions and then filling the weave with an epoxy matrix material. The effective elastic properties of an individual yarn are predicted using a unidirectional (UD) RVE based on the constituent properties of the fiber and matrix materials (see Fig. 3). Then, the woven RVE is meshed by high-fidelity voxel elements, and the elastic analysis is conducted to obtain strain concentration tensor in each element. The degrees of freedom in the woven RVE domain are reduced by clustering these voxel elements based on the strain concentration and orientation in each element. Using the results of the woven RVE clustering, a material database is generated using the method in [32], which includes the interaction tensor, $\mathbf{D}^{IJ}$, the strain concentration tensor of each cluster, $\mathbf{A}^{I}$, the volume fraction, c^{I}, and the material parameters of the individual constituents. In the online stage, a Newton–Raphson iteration algorithm is adopted to solve the discrete incremental Lippmann–Schwinger integral equation set, which can improve the accuracy and convergence, especially for nonlinear material behavior. The solution is the mesoscale strain and stress fields.

2.2. FEM×SCA concurrent multiscale framework

Two scales, the macroscale and mesoscale, are utilized in the concurrent multiscale framework in the paper (Fig. 4). The structural scale (macroscale) is discretized by FEM, which can adapt to complex geometries. The woven RVE scale (mesoscale) is modeled using SCA. A multiscale simulation involving both the macroscale and mesoscale levels is performed in which the information is exchanged concurrently.

The load is applied to the structural scale model. At each integration point in the macroscale elements, the strain increment will be passed from the FEM model in the SCA model. This strain increment is applied to the corresponding woven RVE, and the SCA method is used to solve the woven RVE problem and return the stress increment to the FEM solver. The algorithm for the multiscale simulation of woven composites is summarized in Box I.

From the Box I flowchart, the SCA online algorithm can be implemented by the user-defined subroutine, which can be integrated with most commercial FEM software packages. In this way, the FEM×SCA multiscale framework can be adapted to arbitrary structural geometry and arbitrary woven architecture. Note that the cluster geometry is not required to be regular, which makes it effective for complex microstructure.

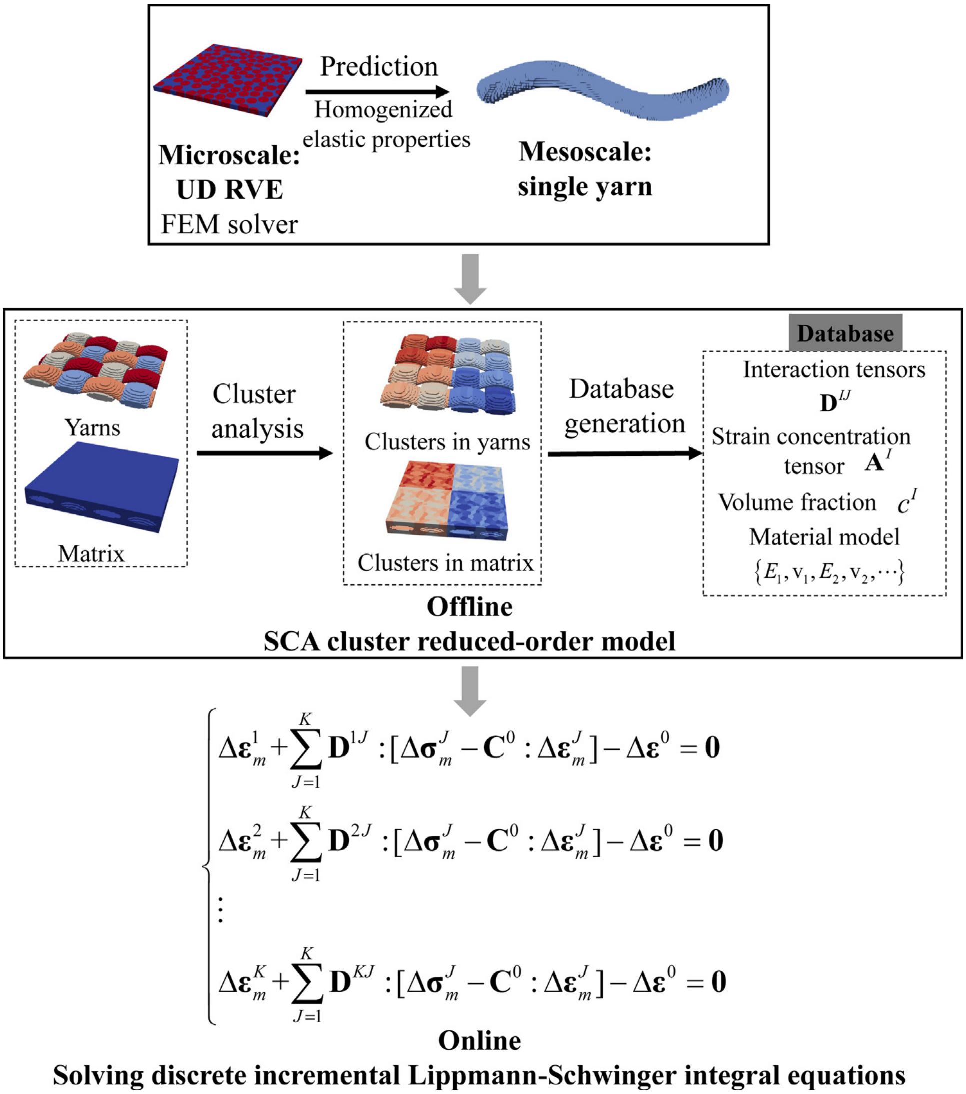

Fig. 3. SCA scheme for woven composites.

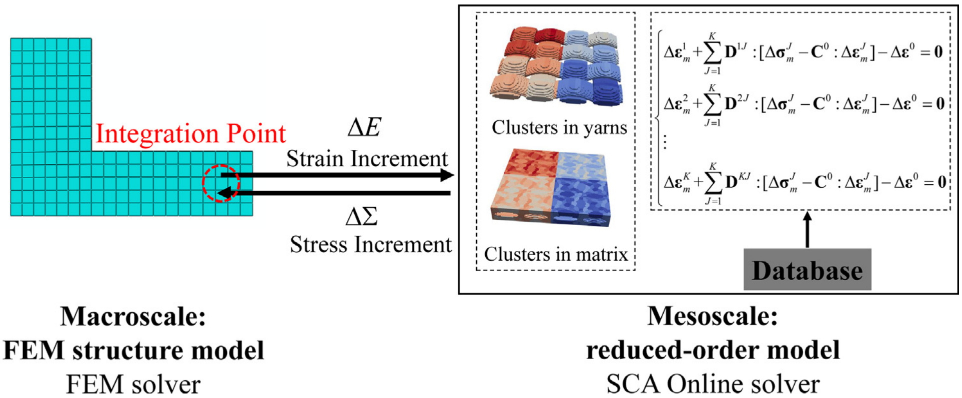

Fig. 4. Concurrent multiscale simulation framework.

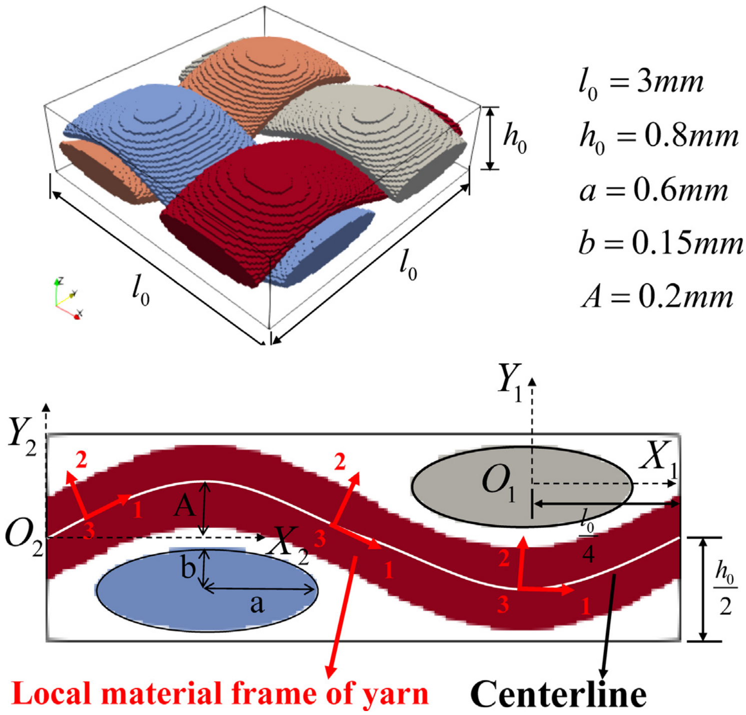

Fig. 5. The microstructure of plain weave composites (three directions in local material frame of yarn, 1: Tangent of the centerline, 2: Vertical to 1 direction, 3: Vertical to 1–2 plane).

3. Verification of SCA for woven RVE

3.1. Geometry model

In the family of woven composites, plain weave composites are widely used for ease of manufacturing. A plain weave composite is selected as an example to demonstrate and verify the SCA method at the RVE level. Fig. 5 shows the plain weave RVE microstructure used in the present work. The cross section of the yarns is assumed to be elliptical, and the centerline of the yarn is modeled as a sine function. Two coordinate systems, $X_1O_1Y_1$ and $X_2O_2Y_2$, are created to describe the cross section and yarn centerline features, respectively. The mathematical description can be shown in Eq. (1). The local coordinate frame 1–2 is used to indicate the local orientation of the yarn, which is also the local system of the material model in yarn. The 1-direction is the tangent of the centerline, and the 2-direction is normal to the 1-direction. This local frame varies along the length of the yarn. The woven RVE used in this paper has 120 voxel elements in both width and length dimensions, and 32 voxel elements in height dimension.

The cross-sectional shape and longitudinal shape are respectively modeled as

$$\begin{cases} \frac{x_1^2}{a^2} + \frac{y_1^2}{b^2} = 1 \\ y_2 = A\sin(\frac{2\pi}{l_0}x_2) \end{cases} \tag{1}$$

where a is long axis, b is short axis of the elliptical cross section respectively, A is amplitude of the sine function in Eq. (1). The three-dimensional geometric model of the woven RVE is defined by five parameters, which are also shown in Fig. 5. The values of these parameters are assumed and are only for numerical verification purposes. With proper experimental characterization, it is possible to generate a realistic woven RVE with these parameters.

Table 1
Material parameters of matrix [37].

Parameter	Value
E (GPa)	3.76
v	0.39
v_{plas}	0.3
σ_{t_0} (MPa)	29
σ_{c_0} (MPa)	67
H_t (MPa)	67
H_c (MPa)	58
n_t	170
n_c	150

Table 2
Material parameters of fiber [38].

	E_1 (GPa)	$E_2 = E_3$ (GPa)	G_{13} (GPa)	v_{12}	v_{23}
Fiber	231	12.97	11.28	0.3	0.45

Table 3
Predicted effective elastic material properties of yarn.

	E_1 (GPa)	$E_2 = E_3$ (GPa)	G_{13} (GPa)	v_{12}	v_{23}
Yarn	138.8	7.08	4.49	0.25	0.31

3.2. Material properties and constitutive model

A nonlinear epoxy plastic material model [36,37] is used to model the polymer matrix. The yield function is written as

$$f(\boldsymbol{\sigma}, \sigma_c, \sigma_t) = 6J_2 + 2I_1(\sigma_c - \sigma_t) - 2\sigma_c\sigma_t \tag{2}$$

where $\boldsymbol{\sigma}$ is Cauchy stress tensor, $I_1 = tr(\boldsymbol{\sigma})$ is the first invariant of Cauchy stress tensor, $J_2 = \frac{1}{2}\boldsymbol{\eta} : \boldsymbol{\eta}$ is the second invariant of deviatoric stress $\boldsymbol{\eta} = \boldsymbol{\sigma} - \frac{1}{3}I_1$, σ_t and σ_c are yield strengths in tension and compression. A non-associative flow rule is used, with the plastic potential function written as

$$\mathrm{g}(\boldsymbol{\sigma}, \sigma_c, \sigma_t) = 6J_2 + 2\alpha I_1(\sigma_c - \sigma_t) - 2\sigma_c\sigma_t \tag{3}$$

where $\alpha = \frac{1-2v_{plas}}{1+v_{plas}}$, v_{plas} is known as plastic Poisson's ratio. Thus, the flow rule is given by

$$\dot{\boldsymbol{\varepsilon}}^p = \dot{\gamma}\frac{\partial g}{\partial \boldsymbol{\sigma}} \tag{4}$$

where $\dot{\gamma}$ represents the time derivative of the plastic multiplier. The evolution of yield strengths in tension and compression are written as

$$\begin{aligned} \sigma_t &= \sigma_{t_0} + H_t(1 - \mathrm{e}^{-n_t\alpha_0}) \\ \sigma_c &= \sigma_{c_0} + H_c(1 - \mathrm{e}^{-n_c\alpha_1}) \end{aligned} \tag{5}$$

where σ_{t_0} and σ_{c_0} are the initial yield strengths in tension and compression, H_t and H_c are hardening parameters in case of tension and compression respectively. These material parameters are given in Table 1. α_0 and α_1 are internal kinematic variables, which are determined by the epoxy experimental data in [37].

A transversely isotropic elastic material model is considered for the fibers. The elastic properties are list in Table 2. The fiber volume fraction is assumed to be 0.60. The subscripts 1, 2 and 3 indicate the local material orientation of yarns in the 1–2–3 frame (see Fig. 5). The UD RVE (Fig. 6) used in this paper has 240 voxel elements in both width and length directions, and 10 voxel elements in height direction.

The effective material properties of the yarn are predicted using a unidirectional (UD) RVE (Fig. 6) model and the elastic properties (Tables 1 and 2) by applying six orthogonal loads with periodic boundary conditions (PBC). As a result, the elastic material properties of yarn are presented in Table 3.

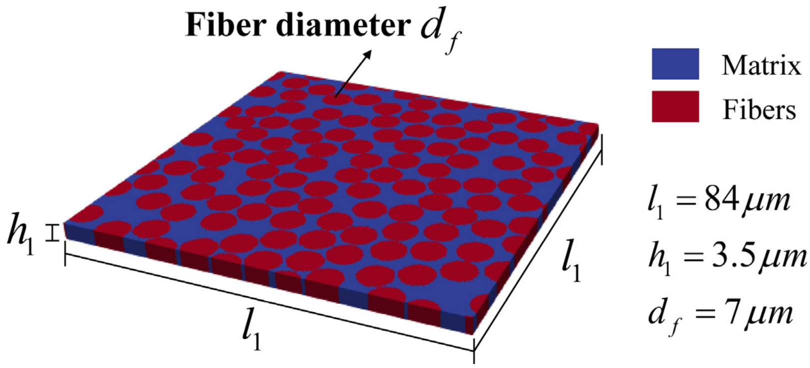

Fig. 6. UD RVE model.

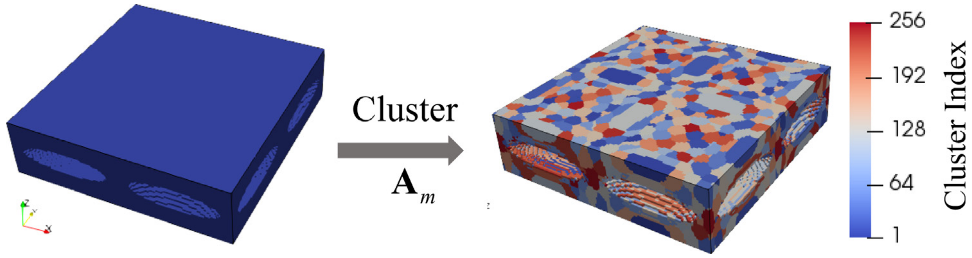

Fig. 7. Clustering process and results of matrix with 256 clusters. Dimensions are given in Fig. 5.

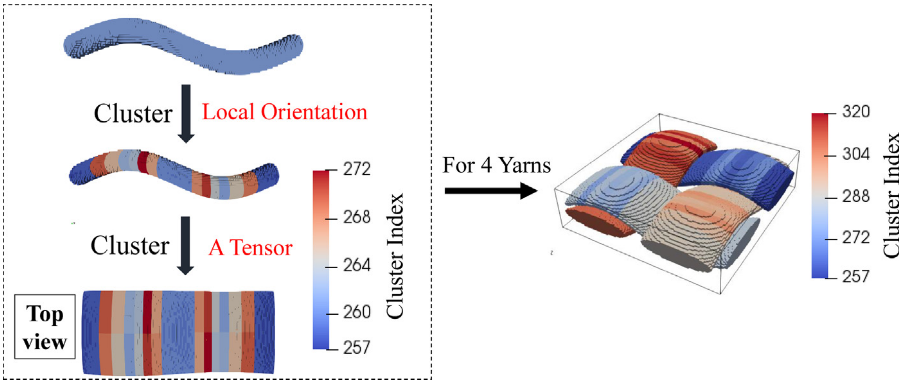

Fig. 8. Clustering process and results of yarns with 64 clusters. For each yarn, clustering is performed first based on local orientation. The resulting clusters are refined further using strain concentration tensor, $\mathbf{A}_{\mathrm{m}}$.

3.3. Clustering process for the woven mesoscale RVE

The matrix material is isotropic, which requires that the clustering only be conducted once, based on the $\mathbf{A}_m$ tensor. After this procedure, the material points with the most similar $\mathbf{A}_m$ tensor will be grouped into the same clusters. Fig. 7. shows the clustering results of the matrix for 256 clusters using k-means clustering.

3.4. Results and discussion

The clustering process for the yarn material will be more complex, as illustrated in Fig. 8. Each cluster corresponds to an orientation-dependent material law, and the local coordinate frame is aligned to the centerline of

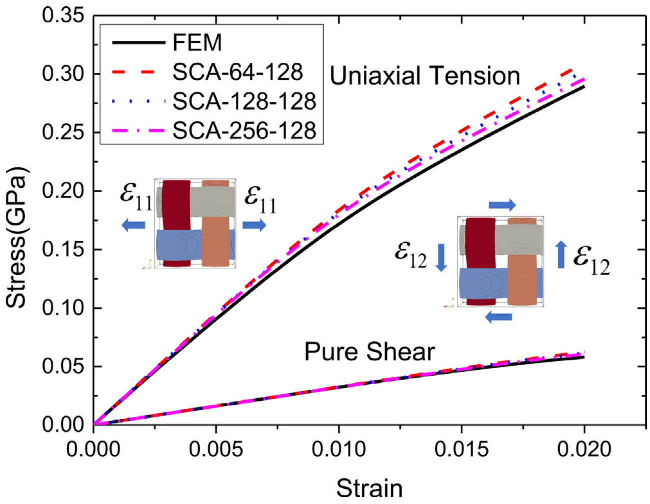

Fig. 9. The prediction results given by FEM and SCA (the SCA-64-128 indicates 64 clusters in matrix and 128 clusters in the yarns).

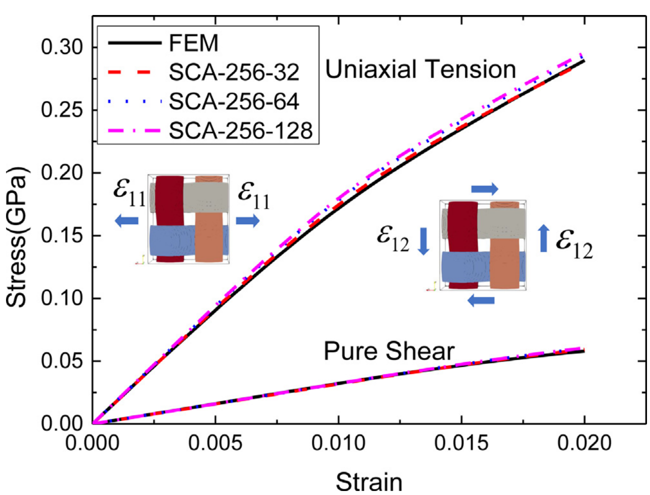

Fig. 10. The prediction results given by FEM and SCA.

the yarn (see Fig. 5). The 1-direction is tangent to the yarn centerline and represents the yarn material orientation for each material point. Clustering is conducted using a two-step process. First, a single yarn is clustered based on the material orientation using k-means. The points with the closest material orientation will clustered together. Based on the results in the first step, the material points in the same cluster will be clustered a second time according to strain concentration tensor, $\mathbf{A}_m$. In this paper, two clusters are used for the second step. After the two-step clustering, the material points with the closest orientation and the closest strain concentration tensor will be grouped into the same cluster. This two-step clustering process is repeated for all yarns in the RVE.

Uniaxial tension and pure shear responses are calculated using the SCA method. Figs. 9–10 include the stress–strain curves for the woven composites under these two different load cases. The number of clusters in the matrix ranges from 64 to 256, while the number of clusters in the yarns is fixed at 128. When the number of clusters in the yarns changes from 32 to 128, the number of clusters in the matrix is fixed to 256. The results from the FEM are also provided as comparison to the baseline solution. It can be concluded that the SCA results are in very good agreement with the FEM results under the pure shear condition in both the linear and nonlinear regions. For the uniaxial tension condition, the SCA results converged with the FEM results as the number of clusters in the matrix

Table 4
Offline computational time of SCA.

	Computational time (s)
SCA-64-128	813
SCA-128-128	1432
SCA-256-128	3571

Table 5
Computation efficiency comparison of FEM and SCA.

	Elements/clusters	DOF	Computational time (s)	
			Uniaxial tension	Pure shear
FEM	460 800	1.45 million	6785.8	6523.1
SCA-64-128	192	1152	11.5	10.4
SCA-128-128	256	1536	18.2	17.8
SCA-256-128	384	2304	28.8	19.8
Max. speed up	2400	1258	590.1	627.2

Table 6
Offline computational time of SCA.

	Computational time (s)
SCA-256-32	1984
SCA-256-64	2416
SCA-256-128	3571

Table 7
Computation efficiency comparison of FEM and SCA.

	Elements/clusters	DOF	Computational time (s)	
			Uniaxial tension	Pure shear
FEM	460 800	1.45 million	6785.8	6523.1
SCA-256-32	288	1728	20.9	14.5
SCA-256-64	320	1920	22.6	17.1
SCA-256-128	384	2304	28.8	19.8
Max. speed up	1600	839	324.7	449.9

increased. Since the nonlinear constitutive model is only used for the matrix material, more clusters are needed to capture the local material nonlinear effects. Compared with the computational cost of FEM, SCA is capable of accurately capturing nonlinear behavior of woven composites with significantly fewer degrees of freedom (SCA results differ by less than 4% compared with FEM using 256 clusters in matrix and 128 clusters in the yarns). Tables 5 and 7 present the efficiency comparison between the FEM and SCA methods. FEM required about 1.45 million DOFs be solved with a solution time of 6523 s, while SCA only requires 2304 DOF and has a solution time of 30 s. The offline stage computational time is provided in Tables 4 and 6. As a result, the SCA method significantly improves computational efficiency in terms of time and memory requirements.

4. Property prediction and concurrent multiscale simulation

4.1. Macroscale anisotropic yield surface prediction

A nonlinear epoxy elastic–plastic material law is considered for the matrix, which results in the overall elastic–plastic behavior for woven RVE. The yield stress of the elastic–plastic material is an important property for material selection and design of composite structures. A yield surface is developed to evaluate material yielding under various loading conditions. The anisotropic Hill yield criterion [39] is considered in this paper for woven composites. The homogenized material law can be efficiently predicted using SCA based on the epoxy elastic–plastic material law for the matrix and the elastic material law for the yarn. The quadratic Hill yield criterion has the following form:

$$F(\sigma_{yy}-\sigma_{zz})^2+G(\sigma_{zz}-\sigma_{xx})^2+H(\sigma_{xx}-\sigma_{yy})^2+2L\sigma_{yz}^2+2M\sigma_{zx}^2+2N\sigma_{xy}^2=1 \tag{6}$$

where F, G, H, L, M, N are constants characteristic of the yield surface, which are traditionally determined by burdensome experiments. Additionally, some experiments are difficult to perform, such as the out-of-plane tension test. In this paper, these parameters are predicted using the SCA method, which significantly reduces the computational cost and improves the efficiency. If Y_{xx}, Y_{yy}, Y_{zz} are the tensile yield stresses in the principal anisotropic direction, it can be shown that:

$$\begin{aligned} \frac{1}{Y_{xx}^2}&=G+H \quad , \quad 2F=\frac{1}{Y_{yy}^2}+\frac{1}{Y_{zz}^2}-\frac{1}{Y_{xx}^2} \\ \frac{1}{Y_{yy}^2}&=H+F \quad , \quad 2G=\frac{1}{Y_{zz}^2}+\frac{1}{Y_{xx}^2}-\frac{1}{Y_{yy}^2} \\ \frac{1}{Y_{zz}^2}&=F+G \quad , \quad 2H=\frac{1}{Y_{xx}^2}+\frac{1}{Y_{yy}^2}-\frac{1}{Y_{zz}^2} \end{aligned} \tag{7}$$

If Y_{yz}, Y_{zx}, Y_{xy} are the yield stresses in shear with respect to the principal axes of anisotropy, then

$$2L=\frac{1}{Y_{yz}^2}, \quad 2M=\frac{1}{Y_{zx}^2}, \quad 2N=\frac{1}{Y_{xy}^2} \tag{8}$$

By taking advantage of the symmetrical features of the woven RVE, only four orthogonal loading conditions are applied to the RVE; the responses are calculated using the SCA method. The tangent stiffness is computed at each point from the stress–strain response, and the yield points are identified by evaluating the change in the tangent stiffness. As a result, the values of yield stress in six directions are obtained. In addition, the Hill constants in Eq. (6) are calculated using Eqs. (7) and (8) using the values of yield stress. The six-dimensional yield surface described by Eq. (6) can be difficult to visualize, but by selecting three components at a time (and setting other three components to be zero), this six-dimensional yield surface is plotted in three-dimensional space (see Fig. 11).

For the nonlinear computation of woven composite structures, this anisotropic Hill yield surface can be used as a criterion to efficiently identify the onset of the plastic deformation under various loading conditions.

The present workflow (Fig. 11) allows one to construct the yield surface for various microstructural and material constitutive information with minimal efforts (approximately one minute on a personal computer). A large woven composite response database can be built to assist design of woven composite against yielding. Given *a priori* information on maximum service loads, the database will provide all possible woven microstructure (e.g. yarn geometry and yarn angle) and material constituents (e.g. matrix properties and yarn properties) that would prevent yielding to occur. Hence, the workflow can accelerate the woven composite design process by efficiently identifying the allowable design space of various design parameters.

4.2. Multiscale simulation convergence study

An RVE convergence study is first conducted to quantify the effect of RVE size on the stress–strain response (Fig. 12). RVE-1 is a unit cell of plain weave woven composite, and RVE-2 is eight times bigger than the RVE-1. The material properties from Section 3.2 are used. The results for these two different RVE sizes are shown in Fig. 12. It is noted that the results are in close agreement with each other (2% difference). Thus, the RVE-1 will provide converged results with greater computational efficiency.

4.3. T-shaped hooking structure analysis

Woven composites are generally made of multiple layers for industrial application. A T-shaped hooking structure [40] is a common geometry for connecting different composite parts. In this example, multiscale simulation is used to capture the macroscale and mesoscale fields in different layers during cyclic bending of the T-shaped hooking structure. The structure and the loading condition are depicted in Fig. 13. Multiple layers are considered through the thickness. The red highlighted area in Fig. 13(b) represents a critical zone when failure stresses are reached, as demonstrated through experiments [40], and a finer mesh is used in this area. The total number of elements is 34,720 for the structural level model.

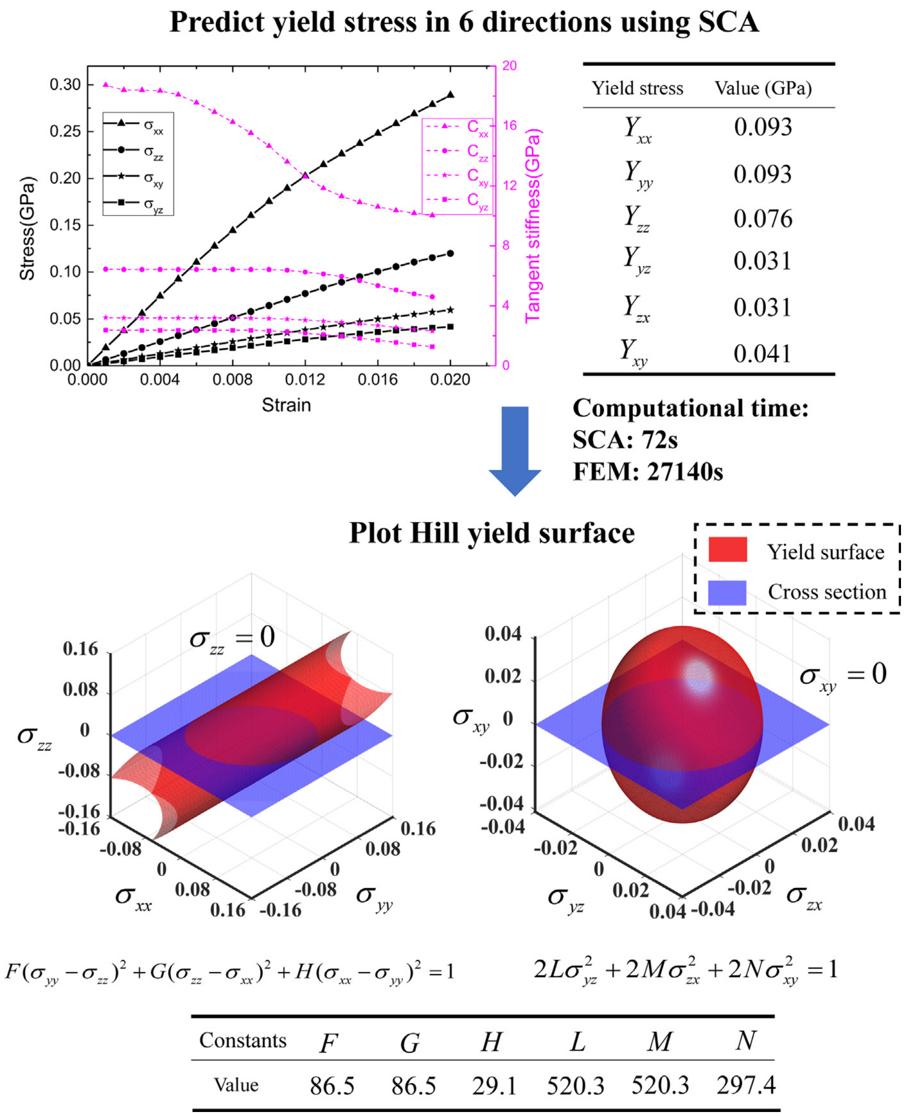

Fig. 11. Hill yield surface calculation workflow. The 3D yield surfaces are plotted against three normal stress components and three shear stress components. For the plot against normal stress components, the cross section where $\sigma_{zz} = 0$ is illustrated. For the plot against shear stress components, the cross section where $\sigma_{xy} = 0$ is plotted.

For woven mesoscale RVE, 64 clusters in the matrix and 32 clusters in the yarns are considered for the SCA calculation, while the eight-node continuum brick element with a reduced integration (ABAQUS element C3D8R) element is used for the FEM calculation. The macroscale behavior is determined by the microstructural morphologies and the mesoscale constitutive equation of each cluster. The SCA material database is first generated during the offline stage, which makes the multiscale simulation more efficient.

This numerical study is implemented with an ABAQUS VUMAT User Subroutine [41] and the discrete incremental Lippmann–Schwinger equations are solved using Intel Math Kernel Library (MKL) FORTRAN codes. This numerical example is run on Intel(R) Xeon(R) processor with 48 cores and 128 GB memory.

The computational results are presented in Fig. 14. Four elements in different layers around the corner are selected to present the mesoscale fields. For the bending loading condition, a stress gradient exists through the thickness, and the stress fields are different in different RVEs. Since the yarns have a much higher modulus, they undertake much more loading than matrix. The homogenized stress–strain curve at maximum stress location is plotted in

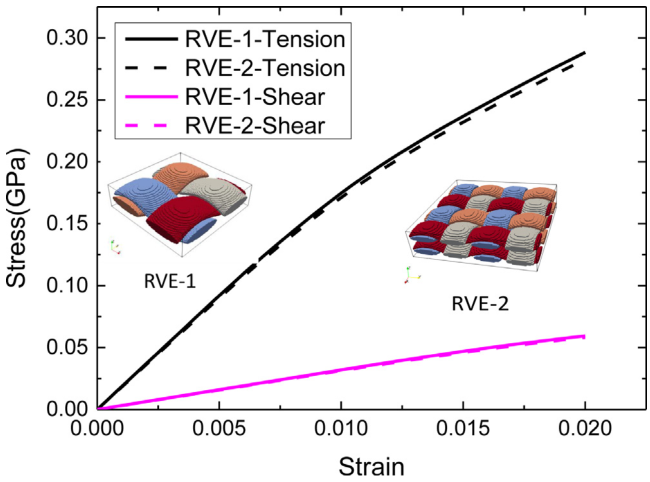

Fig. 12. Convergence study for different RVE sizes.

Table 8
Computational time comparison.

Concurrent multiscale framework	Computational time
FE^2	5.2×10^5days (Estimated)
FEM × SCA	2.4 days
Speed up	**2.16×10^5X**

Fig. 14, which shows the residual plastic strain after loading and unloading. The stress state at peak point is plotted on the 2D yield surface, which shows that the stress has already exceeded the initial yield surface. Additionally, the computational times are presented in Table 8, which demonstrates the significant improvements in efficiency of FEM×SCA framework.

The above numerical study presents the advantages of using the proposed multiscale simulation framework. The stress and strain fields can be captured in both macroscale and mesoscale, including the nonlinear effects, which are difficult to observe using experimental technology. As a result, this framework establishes the connection between the microstructure and macroscale response of the composites structure. When the woven microstructure is modified, but the yarn and matrix material remain unchanged, no additional experiments are needed to calibrate the constitutive equations; only the SCA offline database needs to be updated. In this way, it reduces the cost and improves the efficiency to find the optimal microstructure for the specific structures. Given the efficiency of the SCA online, the larger dimensional composites structures can be analyzed using this framework.

5. Conclusion

In this paper, a woven composite multiscale modeling framework based on Self-consistent Clustering Analysis (SCA) is established. A two-stage reduced order modeling process for woven composite materials using an RVE is developed. In the initial offline data compression stage, a clustering technique is utilized to reduce the overall degrees of freedom in the RVE domain as material points with similar mechanical responses are grouped into clusters. An interaction tensor linking different clusters is then computed, and a woven RVE microstructure database is generated. In the second online stage, Newton–Raphson iteration is used to solve for equilibrium using the reduced-order discrete incremental Lippmann–Schwinger integral equation. This method exhibits rapid convergence for both linear and nonlinear material laws.

The woven multiscale modeling approach provides two attractive features: (1) given the woven microstructure, the online stage can utilize different materials laws for matrix and yarn phases to compute woven microstructure responses. For example, for temperature dependent material properties, the woven behavior at different operation

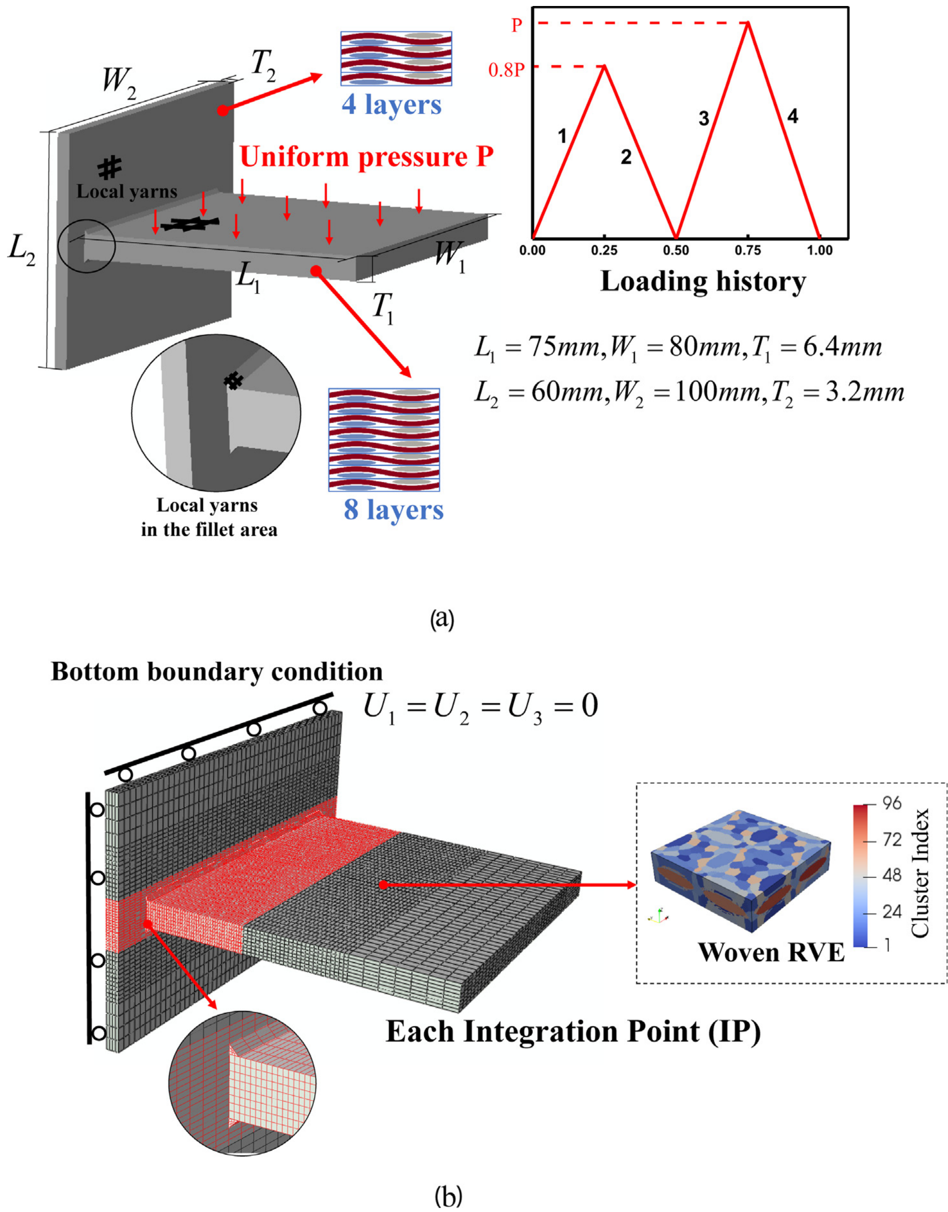

Fig. 13. Geometry and mesh of the T-shaped hooking structure: (a) geometry and boundary conditions, (b) mesh model and reduced order model.

temperature can be computed efficiently. (2) Given the same constituents properties, one only needs to update the offline database to incorporate different weave structures, such as plain weave, twill weave, or satin weave.

The woven multiscale modeling framework has various potential applications, where two important applications are illustrated in the present work:

1. Rapid yield surface generation for woven design against yielding. The yield surface generation workflow can be used to investigate whether the woven composite would experience plastic deformation under possible loading conditions. Note that it can be easily extended to failure surface prediction when the yield analysis is replaced with the failure analysis.

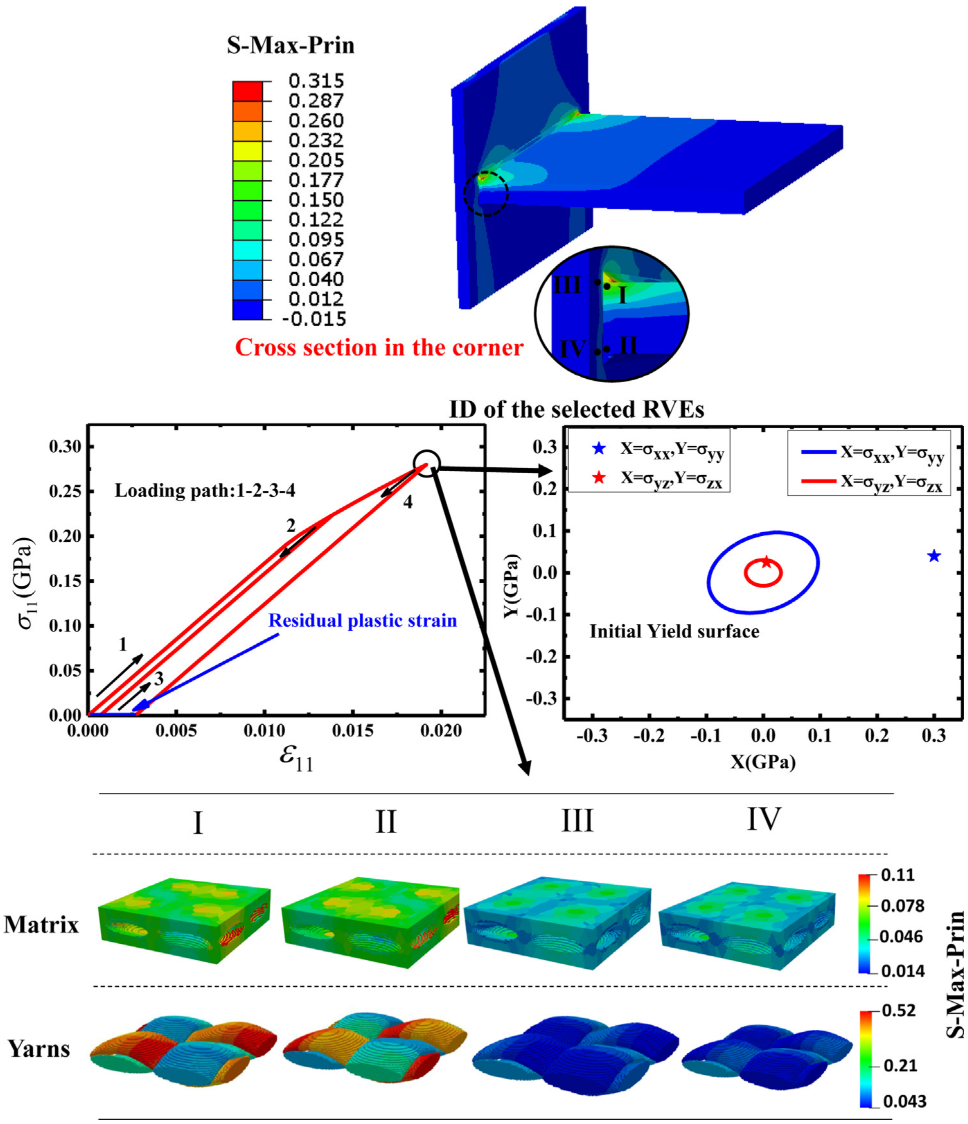

Fig. 14. Simulation results of the T-shaped hooking structure.

2. FEM×SCA concurrent modeling framework of woven laminates which captures macroscale (FEM mesh) and mesoscale mechanical behavior simultaneously during the analysis. The mesoscale field evolution can be tracked as the load increases and the bridge between microstructural and macrostructural response is built. Based on the FEM×SCA framework, the damage and failure model can be incorporated into the mesoscale to provide more detailed analysis, such as conducting composites structure level failure analysis. Compared to the FE^2 framework, the efficiency of concurrent multiscale simulation is significantly improved using FEM×SCA framework. In addition, this framework can be extended to larger scale structure level analysis with complex loading conditions. Finally, this work provides an efficient methodology and framework to solve the woven composites multiscale problems.

Acknowledgments

This research is motivated and initiated from the writing of the US National Science Foundation (NSF) funded proposal under Grant No. MOMS/CMMI-1762035, PI Wing Kam Liu. The US NSF support of this research is greatly appreciated. The first author Xinxing Han warmly acknowledges the financial support of the China Scholarship Council to enable this work. Chenghai Xu , Weihua Xie and Songhe Meng warmly thank the support of National Natural Science Foundation of China (Grant Nos. 11672088), the National Basic Research Program of China (973 Program; Grant No. 2015CB655200) and Science & Technology on Reliability & Environmental Engineering Laboratory, China.

References

[1] A.P. Mouritz, M.K. Bannister, P. Falzon, K. Leong, Manufacturing, review of applications for advanced three-dimensional fibre textile composites, Composites A 30 (1999) 1445–1461.
[2] T. Ishikawa, T.-W. Chou, Stiffness and strength behaviour of woven fabric composites, J. Mater. Sci. 17 (1982) 3211–3220.
[3] H.S. Park, E.G. Karpov, P.A. Klein, W.K. Liu, Three-dimensional bridging scale analysis of dynamic fracture, J. Comput. Phys. 207 (2005) 588–609.
[4] H. Kadowaki, W.K. Liu, Bridging multi-scale method for localization problems, Comput. Methods Appl. Mech. Eng. 193 (2004) 3267–3302.
[5] G.J. Wagner, W.K. Liu, Coupling of atomistic and continuum simulations using a bridging scale decomposition, J. Comput. Phys. 190 (2003) 249–274.
[6] V. Kouznetsova, M.G. Geers, W.M. Brekelmans, Multi-scale constitutive modelling of heterogeneous materials with a gradient-enhanced computational homogenization scheme, Internat. J. Numer. Methods Engrg. 54 (2002) 1235–1260.
[7] F. Feyel, J.-L. Chaboche, FE2 multiscale approach for modelling the elastoviscoplastic behaviour of long fibre SiC/Ti composite materials, Comput. Methods Appl. Mech. Eng. 183 (2000) 309–330.
[8] J. Gao, B. Liang, W. Zhang, Z. Liu, P. Cheng, R. Bostanabad, J. Cao, W. Chen, W.K. Liu, X. Su, Multiscale modeling of carbon fiber reinforced polymer (CFRP) for integrated computational materials engineering process, in: Ford Motor Company, 2017.
[9] R. Bostanabad, B. Liang, J. Gao, W.K. Liu, J. Cao, D. Zeng, X. Su, H. Xu, Y. Li, W. Chen, Uncertainty quantification in multiscale simulation of woven fiber composites, Comput. Methods Appl. Mech. Eng. 338 (2018) 506–532.
[10] T. Kanit, S. Forest, I. Galliet, V. Mounoury, D. Jeulin, Determination of the size of the representative volume element for random composites: statistical and numerical approach, Int. J. Solids Struct. 40 (2003) 3647–3679.
[11] Y.J. Liu, X.L. Chen, Evaluations of the effective material properties of carbon nanotube-based composites using a nanoscale representative volume element, Mech. Mater. 35 (2003) 69–81.
[12] C.T. Sun, R.S. Vaidya, Prediction of composite properties, from a representative volume element, Compos. Sci. Technol. 56 (1996) 171–179.
[13] X.L. Chen, Y.J. Liu, Square representative volume elements for evaluating the effective material properties of carbon nanotube-based composites, Comput. Mater. Sci. 29 (2004) 1–11.
[14] Z.H. Xia, Y.F. Zhang, F. Ellyin, A unified periodical boundary conditions for representative volume elements of composites and applications, Int. J. Solids Struct. 40 (2003) 1907–1921.
[15] Z. Liu, J.A. Moore, W.K. Liu, An extended micromechanics method for probing interphase properties in polymer nanocomposites, J. Mech. Phys. Solids 95 (2016) 663–680.
[16] T. Mura, Micromechanics of Defects in Solids, Springer Science & Business Media, 2013.
[17] R. Hill, A self-consistent mechanics of composite materials, J. Mech. Phys. Solids 13 (1965) 213–222.
[18] J.D. Eshelby, The determination of the elastic field of an ellipsoidal inclusion, and related problems, Proc. R. Soc. Lond. Ser. A Math. Phys. Eng. Sci. 241 (1957) 376–396.
[19] W. Zhang, H. Ren, B. Liang, D. Zeng, X. Su, J. Dahl, M. Mirdamadi, Q. Zhao, J. Cao, A non-orthogonal material model of woven composites in the preforming process, CIRP Ann. 66 (2017) 257–260.
[20] J.-C. Michel, H. Moulinec, P. Suquet, Effective properties of composite materials with periodic microstructure: a computational approach, Comput. Methods Appl. Mech. Eng. 172 (1999) 109–143.
[21] H. Moulinec, P. Suquet, A numerical method for computing the overall response of nonlinear composites with complex microstructure, Comput. Methods Appl. Mech. Eng. 157 (1998) 69–94.
[22] G. Dvorak, A. Wafa, Y. Bahei-El-Din, Implementation of the transformation field analysis for inelastic composite materials, Comput. Mech. 14 (1994) 201–228.
[23] G. Dvorak, Transformation field analysis of inelastic composite materials, Proc. R. Soc. Lond. Ser. A Math. Phys. Eng. Sci. 437 (1992) 311–327.
[24] S. Roussette, J.-C. Michel, P. Suquet, Nonuniform transformation field analysis of elastic–viscoplastic composites, Compos. Sci. Technol. 69 (2009) 22–27.
[25] J.-C. Michel, P. Suquet, Computational analysis of nonlinear composite structures using the nonuniform transformation field analysis, Comput. Methods Appl. Mech. Eng. 193 (2004) 5477–5502.
[26] J.-C. Michel, P. Suquet, Nonuniform transformation field analysis, Int. J. Solids Struct. 40 (2003) 6937–6955.
[27] P. Ladevèze, J.-C. Passieux, D. Néron, The latin multiscale computational method and the proper generalized decomposition, Comput. Methods Appl. Mech. Eng. 199 (2010) 1287–1296.
[28] K. Willcox, J. Peraire, Balanced model reduction via the proper orthogonal decomposition, Aiaa J 40 (2002) 2323–2330.
[29] A. Chatterjee, An introduction to the proper orthogonal decomposition, Current Sci. (2000) 808–817.
[30] G. Berkooz, P. Holmes, J.L. Lumley, The proper orthogonal decomposition in the analysis of turbulent flows, Annu. Rev. Fluid Mech. 25 (1993) 539–575.

[31] I. Özdemir, W. Brekelmans, M.G. Geers, FE2 computational homogenization for the thermo-mechanical analysis of heterogeneous solids, Comput. Methods Appl. Mech. Eng. 198 (2008) 602–613.
[32] Z.L. Liu, M.A. Bessa, W.K. Liu, Self-consistent clustering analysis: An efficient multi-scale scheme for inelastic heterogeneous materials, Comput. Methods Appl. Mech. 306 (2016) 319–341.
[33] Z. Liu, M. Fleming, W.K. Liu, Microstructural material database for self-consistent clustering analysis of elastoplastic strain softening materials, Comput. Methods Appl. Mech. Eng. 330 (2018) 547–577.
[34] Z. Liu, O.L. Kafka, C. Yu, W.K. Liu, Data-driven self-consistent clustering analysis of heterogeneous materials with crystal plasticity, in: Advances in Computational Plasticity, Springer, 2018, pp. 221–242.
[35] M. Bessa, R. Bostanabad, Z. Liu, A. Hu, D.W. Apley, C. Brinson, W. Chen, W.K. Liu, A framework for data-driven analysis of materials under uncertainty: Countering the curse of dimensionality, Comput. Methods Appl. Mech. Eng. 320 (2017) 633–667.
[36] A. Melro, P. Camanho, F.A. Pires, S. Pinho, Micromechanical analysis of polymer composites reinforced by unidirectional fibres: Part I–Constitutive modelling, Int. J. Solids Struct. 50 (2013) 1897–1905.
[37] Z. Ullah, L. Kaczmarczyk, C.J. Pearce, Three-dimensional nonlinear micro/meso-mechanical response of the fibre-reinforced polymer composites, Compos. Struct. 161 (2017) 204–214.
[38] F. Naya, C. González, C. Lopes, S. Van der Veen, F. Pons, Manufacturing, computational micromechanics of the transverse and shear behavior of unidirectional fiber reinforced polymers including environmental effects, Composites A 92 (2017) 146–157.
[39] R. Hill, A theory of the yielding and plastic flow of anisotropic metals, Proc. R. Soc. Lond. Ser. A Math. Phys. Eng. Sci. 193 (1948) 281–297.
[40] H. Zhang, J. Guo, W. Wen, H. Cui, S. He, Y. Xu, Bending/tensile tests and simulations of the 2.5 D woven T-shaped hooking composite structure, Compos. Struct. 206 (2018) 155–163.
[41] D.J.A.U.S.R.M. Systèmes, Abaqus 6.10 online documentation, 2010.